Title: A single nuclei transcriptomic analysis of the Atlantic salmon gill through smoltification and seawater transfer

Authors: Alexander C. West[1], Yasutaka Mizoro[2], Shona H. Wood[1], Louise M. Ince[3], Marianne Iversen[1], Even H. Jørgensen[1], Torfinn Nome[4], Simen Rød Sandve[4], Andrew S. I. Loudon[2] and David G. Hazlerigg[1]

[1]Arctic Chronobiology and Physiology, University of Tromsø, Framstredet 42, 9019 Tromsø, Norway

[2]Division of Diabetes, Endocrinology & Gastroenterology, School of Medical Sciences, Faculty of Biology, Medicine and Health, University of Manchester, UK

[3]University of Geneva, Centre Médical Universitaire (CMU), Department of Pathology and Immunology, Switzerland

[4]Centre for Integrative Genetics, Department of Animal and Aquaculture Sciences, Norwegian University of Life Sciences, 1432 Ås, Norway

*Correspondence: david.hazlerigg@uit.no

Abstract

Anadromous salmonids begin life adapted to the freshwater environments of their natal streams before a developmental transition, known as smoltification, transforms them into marine-adapted fish. In the wild, the extending photoperiods of spring stimulates smoltification, typified by radical reprogramming of the gill from an ion-absorbing organ to ion-excreting organ. Prior work has highlighted the role of specialized “mitochondrion-rich”

cells in delivering this phenotype. However, transcriptomic studies identify thousands of smoltification-driven differentially regulated genes, indicating that smoltification causes a multifaceted, multicellular change; but direct evidence of this is lacking.

Here, we use single-nuclei RNAseq to characterize the Atlantic salmon gill during smoltification and seawater transfer. We identify 20 distinct clusters of nuclei, including known, but also novel gill cell types. These data allow us to isolate cluster-specific, smoltification-induced changes in gene expression. We also show how cellular make-up of the gill changes through smoltification. As expected, we noted an increase in the proportion of seawater mitochondrion-rich cells, however, we also identify a reduction of several immune-related cells. Overall, our results provide unrivaled detail of the cellular complexity in the gill and suggest that smoltification triggers unexpected immune reprogramming directly preceding seawater entry.

Keywords: Atlantic salmon, smoltification, photoperiod, seasonal, gill

Introduction

The Atlantic salmon migrates between fresh and seawater environments [1]. Atlantic salmon eggs hatch in freshwater streams where they develop for 1-4 years. On reaching a critical size threshold, young “parr” animals are sensitized by several weeks of winter photoperiod (day-lengths), after which long, summer-like photoperiods stimulates the parr to transform into a marine-adapted “smolt” fish [2]. This process, known as smoltification, drives divergent expression of endocrine factors that collectively deliver phenotypic remodeling, of length, weight, silvering, and in particular: gill physiology [1].

The salmonid gill is a complex multifunctional organ, essential for gas exchange, nitrogenous waste excretion, pH balance and osmoregulation [3]. It is also a major mucosal immune barrier harboring a dedicated lymphoid tissue [4]. Structurally, the gills are arranged in symmetrical arches, each of which are populated by numerous filament structures, which are themselves densely flanked with lamellae. The gill is composed of seven major cell types [5]. Pavement cells (PVCs) have an enlarged surface area on the apical membrane, and form the majority of the epithelium [6]. Pillar cells (PCs), which are structural cells, define the blood spaces within the lamellae [7]. Goblet cells (GCs) reside in the filament epithelium and excrete mucus [8]. Non-differentiated progenitor cells (NDCs) colonize basal and intermediate layers of the gill epithelium [9]. Chemosensory neuroepithelial cells (NECs) lie along the length of the efferent edge of the gills and are innervated by the central nervous system [10]. Mitochondrion-rich cells (MRCs) and their adjacent accessory cells (ACs), finally, are located at the trough between two lamellae where they abundantly express the channels and pumps required to maintain the osmotic gradients between blood plasma and both fresh- and seawater [11–13].

Under freshwater, Na^+ ions are directly or indirectly exchanged for protons across the apical membrane then transported into the blood *via* the sodium potassium ATPase (NKA) on the basolateral membrane [14–16]. Cl^- ions, meanwhile, are exchanged or channeled across the apical membrane then enter the blood through an undefined channel [17–20]. Under saltwater, basolateral NKA generates a chemical and electrical gradient, motivating both loss of Cl^- ions *via* apical CFTR channels and paracellular escape of Na^+ ions [13,21] (reviewed in [22]).

Smoltification converts the Atlantic salmon gill from a freshwater-adapted organ to a seawater-adapted organ. Rising cortisol and growth hormone along with falling prolactin propels smoltification. This change in endocrinology coincides with a switch in anatomical and

67 molecular phenotypes of MRCs and ACs, cell types which to date comprise the major focus of
68 smoltification of gill physiology [1,12,23]. Smoltification is, however, a complex developmental
69 transition and the smolt gill phenotype likely extends far beyond changing MRC and AC cell
70 phenotype. Therefore, to realize the complexities of smoltification-driven changes in gill
71 physiology we adopt a new strategy, single-nuclei RNAseq, which provides transcriptional
72 responses to smoltification and seawater transfer at individual nuclei-level resolution.

73 **Results & Discussion**

74 **A single-nuclei survey of Atlantic salmon gill cells**

75 We profiled 18,844 individual nuclei from eight Atlantic salmon gill samples from four distinct
76 physiological states (Figure 1A). To define shared correlation structure across datasets we
77 pooled replicate samples and integrated all four states using diagonalized canonical
78 correlation analysis followed by L2 normalization. We next identified pairs of mutual nearest
79 neighbors (MNNs) to identify anchors: cells that represent shared biological states across
80 datasets. Anchors were then used to calculate "correction" vectors allowing all fours states to
81 be jointly analyzed as an integrated reference [24]. Unsupervised graph clustering partitioned
82 the nuclei into 20 clusters, which we visualized using a uniform manifold approximation and
83 projection (UMAP) dimension reduction technique (Figure 1B).

84 Lists of co-expressed marker genes define individual clusters. We categorized
85 individual clusters using gene ontology analysis of marker gene lists and unique expression of
86 known marker genes. This approach allowed us to infer cell types including fresh- and
87 seawater MRCs, ACs, neuroendothelial cells, goblet cells, non-differentiated cells, pillar cells,
88 lymphatic endothelial cells and several types of blood cell. We also identified a novel
89 population of fibrocyte-like cells, and several types of vascular- and endothelial-like cells that

partitioned across several clusters, together suggesting greater complexity in gill cytology that previously appreciated (Figure 1B).

We then defined expression signatures for each cell cluster. Our analysis re-identified several known marker genes, but also identifying several novel cell-type markers (Figure 1C). For example, the accessory cell signature included highly restricted expression of Slc26a6, an apical membrane Cl^-/HCO_3 exchanger, associated with gill function but until now misattributed to expression within MRCs [25,26]. We were interested to note that the markers defining the erythrocyte population, including beta-globin, were expressed widely among all cell types. It is unclear exactly what role extra-erythroid haemoglobin plays in the gill, however, mammalian studies suggest that haemoglobin, in addition to its oxygen carrying capacity, may play an antimicrobial role [27]. As a major mucosal immune barrier, this capacity may be pertinent to the gill [28].

Major changes in cell composition during smoltification

To understand how gene expression and cellular complexity changes within the gill during smoltification and seawater transfer we compared the snRNAseq profiles at different developmental points (Fig 2A, for confirmation of smolt status see[29]). The abundance of six nuclei clusters changed dramatically (>3 fold change in percentage abundance) during smoltification (Figure 2B). SW MRCs increased in proportion steadily from T1-T4, consistent with previous descriptions of Atlantic salmon gill physiology. We also observed a marked increase in vascular cell number, with the major differences occurring between T2 and T3, suggesting that this vascular cell cluster proliferate in line with growth rates (Figure 2C). Interestingly, four immune-related nuclei clusters representing T cells, myeloid cells, dendritic cells and lymphatic endothelial cells fell dramatically during smoltification (Figure 2D).

Changes in cell abundance occurred with a similar profile in all immune-associated cell clusters, with consistent decline observed between T1-T3. In contrast, 24h SW transfer does not appear to affect immune-cell abundance directly. These results highlight the complex and dynamic changes in cellular composition that occur in the gill during smoltification.

Cell cluster-specific expression of smoltification-associated factors

Next, we wanted to identify cluster types where smoltification drives changes in local gene regulation. For statistical power, we cross-referenced our snRNAseq analysis with whole gill RNAseq analysis of T1-T3, identifying 9746 genes differentially regulated by smoltification (FDR <0.01). Pearson clustering of these genes resolved five major clusters that were associated with immune response, structural morphogenesis, autophagy, catabolism and mitochondrial respiration (Figure 3A). Within our analysis we identified a number of "classical" smoltification-related genes. As expected, CFTR was highest under constant light (LL), and was highly localized in expression to MRCs (Figure 3B). We also identified the reciprocal regulation of sodium-potassium ATPase subunits, specifically, suppression of NKAa1a and increase in NKAa1b [12]. Inspection of cellular localization within our snRNAseq dataset showed that expression of these genes were, as anticipated, highest within the MRCs and ACs (Figure 3B).

Our previous work identified genes whose expression are predicated on exposure to several weeks of short-photoperiod exposure[29]. In Atlantic salmon, these "winter-dependent" genes are analogous to vernalization dependent genes in *Arabidopsis*[30], where a dosage of exposure to a winter-like stimulus (in *Arabidopsis*, cold; in Atlantic salmon, short photoperiod) controls the presentation of a seasonal phenotype under summer-like stimulus (in *Arabidopsis*, warmth and long days; in Atlantic salmon, long photoperiod). Winter-dependent genes are therefore intrinsically linked to unidirectional smolt development, and may play a

mechanistic role in pre-adaptation of the gill for seawater migration. Surprisingly, canonical markers of smolt status, including the reciprocal expression of NKA subunits, are not winter dependent, meaning that their expression is passive to photoperiod rather than life history progression[29].

Using our RNAseq dataset we identified novel, winter dependent genes. Next, we mined our snRNAseq dataset to identify the cell clusters that express these factors (Figure S1). Of particular interest was Cuzd1, a gene associated with carcinogenesis, whose expression was tightly localized to non-differentiated cells [31]. We also identified Rhag, an ammonium transporter thought to be erythrocyte specific in mammals, but here predominantly expressed in the vascular cell (VC 3) cluster [32]; and Hg2a (CD74) a ubiquitously expression multi-functional protein linked to immune defense [33]. Taken together our data show that smoltification engages all gill cells in diverse regulatory phenotypes.

Cell cluster-specific expression of seawater transfer-associated factors

Smoltification manifests when the Atlantic salmon smolts migrate downstream and arrive in the marine environment, thereby committing to an oceanic life [1]. To gain insight into this critical step we compared RNA profiles of gill samples between smolts in freshwater and 24h in seawater using whole gill RNAseq, identifying 144 induced and 107 suppressed genes (FDR<0.01). Gene ontologies showed that the induced gene cohort was significantly associated with keratinization, whereas the suppressed gene cohort related to immune function (Figure 4A). We cross-referenced our whole gill RNAseq data against our snRNAseq data to isolate cell-type specificity of gene expression. These data highlight the restricted expression of key up-regulated genes (Figure 4B). For example, we localize the expression of an enzyme involved in both ionic and acid/base balance, carbonic anhydrase, to MRCs [34,35].

We also show that ATP-binding cassette sub-family A member 12 (Abca12), a gene important in epidermal lipid barrier formation [36], is broadly expressed, but particularly concentrated in MRCs (SW), pavement, vascular, and non-differentiated cells. Interestingly, we show that a protein chaperone that helps regulate chromatin state, nucleoplasmin [37,38], is expressed specifically in non-differentiated, vascular and pavement cells groups, suggesting that these cell types undergo a change in chromatin status under seawater exposure.

Conclusions

Our results bring insightful cellular resolution to the complexity of the Atlantic salmon gill and the compositional changes that occur during smoltification. Of particular interest was the suppression of immune cell types, which correlates with reduction in immune-related genes and suppression of immune function during smoltification [39–41]. These data are a puzzle. The marine environment is awash with parasites, bacteria and viruses to which the salmon is potentially vulnerable, so loss of immune function would make little sense. Future work should focus on why and how the immune system is affected in aquaculture. Conceivably these data point towards an adaptive immunological reprogramming that helps to avoid immune shock when the salmon transition between the distinctive pathogen complements of fresh- and seawater habitats [42,43]. Alternatively, artificial smolt production may drive abnormal immunosuppression. The constant light routinely used to stimulate smolts would profoundly undermine the immune defenses of mammals *via* disruption of the circadian clock [44].

Our data also shows that smoltification-driven transcriptional regulation occurs not only in MRCs and ACs, but also in other distinctive cell types including pavement cells, vascular cells and non-differentiated cells. We anticipate that novel gene function within the context

of cell function will be a priority for future investigation, and will be assisted by the novel suite of marker genes which we present here.

References

1. Stefansson, S. O., Björnsson, B. T., Ebbesson, L. O. E. & McCormick, S. D. Smoltification. in *Fish Larval Physiology* 639–681 (2008).

2. Strand, J. E. T., Hazlerigg, D. & Jørgensen, E. H. Photoperiod revisited: is there a critical day length for triggering a complete parr–smolt transformation in Atlantic salmon Salmo salar? *J. Fish Biol.* **93**, 440–448 (2018).

3. Evans, D. H., Piermarini, P. M. & Choe, K. P. The multifunctional fish gill: Dominant site of gas exchange, osmoregulation, acid-base regulation, and excretion of nitrogenous waste. *Physiol. Rev.* **85**, 97–177 (2005).

4. Koppang, E. O. *et al.* Salmonid T cells assemble in the thymus, spleen and in novel interbranchial lymphoid tissue. *J. Anat.* **217**, 728–739 (2010).

5. Wilson, J. M. & Laurent, P. Fish gill morphology: Inside out. *J. Exp. Zool.* **293**, 192–213 (2002).

6. Laurent, P. & Dunel-Erb, S. *The Pseudobranch: Morphology and Function*. *Fish Physiology* vol. 10 (1984).

7. Newstead, J. D. Fine structure of the respiratory lamellae of teleostean gills. *Zeitschrift für Zellforsch. und Mikroskopische Anat.* **79**, 396–428 (1967).

8. Rojo, M. C., Blánquez, M. J. & González, M. E. A histochemical study of the distribution

of lectin binding sites in the developing branchial area of the trout Salmo trutta. *J. Anat.* **189**, 609–621 (1996).

9. Laurent, P., Dunel-Erb, S., Chevalier, C. & Lignon, J. Gill epithelial cells kinetics in a freshwater teleost, Oncorhynchus mykiss during adaptation to ion-poor water and hormonal treatments. *Fish Physiol. Biochem.* **13**, 353–370 (1994).

10. Dunel-Erb, S., Chevalier, C. & Laurent, P. Distribution of neuroepithelial cells and neurons in the trout gill filament: comparison in spring and winter. *Can. J. Zool.* **72**, 1794–1799 (1994).

11. Hootman, S. R. & Philpott, C. W. Accessory cells in teleost branchial epithelium. *Am. J. Physiol. - Regul. Integr. Comp. Physiol.* **7**, (1980).

12. Mccormick, S. D., Regish, A. M., Christensen, A. K. & Björnsson, B. T. Differential regulation of sodium – potassium pump isoforms during smolt development and seawater exposure of Atlantic salmon. 1142–1151 (2013) doi:10.1242/jeb.080440.

13. Sardet, C., Pisam, M. & Maetz, J. The surface epithelium of teleostean fish gills. *J. Cell Biol.* **80**, 96–117 (1979).

14. Edwards, S. L., Tse, C. M. & Toop, T. Immunolocalisation of NHE3-like immunoreactivity in the gills of the rainbow trout (Oncorhynchus mykiss) and the blue-throated wrasse (Pseudolabrus tetrious). *J. Anat.* **195**, 465–469 (1999).

15. Yan, J. J., Chou, M. Y., Kaneko, T. & Hwang, P. P. Gene expression of Na+/H+ exchanger in zebrafish H+-ATPase-rich cells during acclimation to low-Na+ and acidic environments. *Am. J. Physiol. - Cell Physiol.* **293**, 1814–1823 (2007).

16. Hirata, T. *et al.* Mechanism of acid adaptation of a fish living in a ph 3.5 lake. *Am. J.*

Physiol. - Regul. Integr. Comp. Physiol. **284**, (2003).

17. Hiroi, J., McCormick, S. D., Ohtani-Kaneko, R. & Kaneko, T. Functional classification of mitochondrion-rich cells in euryhaline Mozambique tilapia (Oreochromis mossambicus) embryos, by means of triple immunofluorescence staining for Na+/K+-ATPase, Na +/K+/2Cl- cotransporter and CFTR anion channel. *J. Exp. Biol.* **208**, 2023–2036 (2005).

18. Hiroi, J., Yasumasu, S., McCormick, S. D., Hwang, P. P. & Kaneko, T. Evidence for an apical Na-Cl cotransporter involved in ion uptake in a teleost fish. *J. Exp. Biol.* **211**, 2584–2599 (2008).

19. Tang, C. H., Hwang, L. Y. & Lee, T. H. Chloride channel CLC-3 in gills of the euryhaline teleost, tetraodon nigroviridis: Expression, localization and the possible role of chloride absorption. *J. Exp. Biol.* **213**, 683–693 (2010).

20. Preest, M. R., Gonzalez, R. J. & Wilson, R. W. A pharmacological examination of Na+ and Cl- transport in two species of freshwater fish. *Physiol. Biochem. Zool.* **78**, 259–272 (2005).

21. Marshall, W. S., Lynch, E. M. & Cozzi, R. R. F. Redistribution of immunofluorescence of CFTR anion channel and NKCC cotransporter in chloride cells during adaptation of the killifish Fundulus heteroclitus to sea water. *J. Exp. Biol.* **205**, 1265–1273 (2002).

22. Evans, D. H. Freshwater fish gill ion transport: August Krogh to morpholinos and microprobes. *Acta Physiol. (Oxf).* **202**, 349–359 (2011).

23. Lorgen, M. *et al.* Functional divergence of type 2 deiodinase paralogs in the Atlantic salmon. *Curr. Biol.* **25**, 936–941 (2015).

246 24. Stuart, T. *et al.* Comprehensive Integration of Single-Cell Data. *Cell* **177**, 1888-
247 1902.e21 (2019).

248 25. Leguen, I., Le Cam, A., Montfort, J., Peron, S. & Fautrel, A. Transcriptomic analysis of
249 trout gill ionocytes in fresh water and sea water using laser capture microdissection
250 combined with microarray analysis. *PLoS One* **10**, 1–22 (2015).

251 26. Boyle, D., Clifford, A. M., Orr, E., Chamot, D. & Goss, G. G. Mechanisms of Cl- uptake in
252 rainbow trout: Cloning and expression of slc26a6, a prospective Cl-/HCO3- exchanger.
253 *Comp. Biochem. Physiol. -Part A Mol. Integr. Physiol.* **180**, 43–50 (2015).

254 27. Saha, D. *et al.* Hemoglobin Expression in Nonerythroid Cells: Novel or Ubiquitous? *Int.*
255 *J. Inflam.* **2014**, (2014).

256 28. Koppang, E. O., Kvellestad, A. & Fischer, U. *Mucosal Health in Aquaculture Fish*
257 *mucosal immunity: gill*. *Mucosal Health in Aquaculture* (Elsevier Inc., 2015).
258 doi:10.1016/B978-0-12-417186-2/00005-4.

259 29. Iversen, M. *et al.* RNA profiling identifies novel, photoperiodhistory dependent
260 markers associated with enhanced saltwater performance in juvenile Atlantic salmon.
261 *PLoS One* **15**, 1–21 (2020).

262 30. Song, J., Angel, A., Howard, M. & Dean, C. Vernalization - a cold-induced epigenetic
263 switch. *J. Cell Sci.* **125**, 3723–3731 (2012).

264 31. Liaskos, C., Rigopoulou, E. I., Orfanidou, T., Bogdanos, D. P. & Papandreou, C. N.
265 CUZD1 and Anti-CUZD1 Antibodies as Markers of Cancer and Inflammatory Bowel
266 Diseases. **2013**, (2013).

267 32. Tilley, L. *et al.* A new blood group system , RHAG : three antigens resulting from amino

acid substitutions in the Rh-associated glycoprotein. 151–159 (2010) doi:10.1111/j.1423-0410.2009.01243.x.

33. Su, H., Na, N., Zhang, X. & Zhao, Y. The biological function and significance of CD74 in immune diseases. *Inflamm. Res.* **66**, 209–216 (2017).

34. Houde, A. L. S. *et al.* Salmonid gene expression biomarkers indicative of physiological responses to changes in salinity and temperature, but not dissolved oxygen. *J. Exp. Biol.* **222**, (2019).

35. Zbanyszek, R. & Smith, L. S. Changes in carbonic anhydrase activity in coho salmon smolts resulting from physical training and transfer into seawater. *Comp. Biochem. Physiol. -- Part A Physiol.* **79**, 229–233 (1984).

36. Akiyama, M. The roles of ABCA12 in epidermal lipid barrier formation and keratinocyte differentiation. *Biochim. Biophys. Acta - Mol. Cell Biol. Lipids* **1841**, 435–440 (2014).

37. Bouleau, A. *et al.* Maternally inherited npm2 mRNA is crucial for egg developmental competence in zebrafish. *Biol. Reprod.* **91**, 1–9 (2014).

38. Chen, P. *et al.* Nucleoplasmin is a limiting component in the scaling of nuclear size with cytoplasmic volume. *J. Cell Biol.* **218**, 4063–4078 (2019).

39. Jensen, I., Overrein, M. C., Fredriksen, B. N., Strandskog, G. & Seternes, T. Differences in smolt status affect the resistance of Atlantic salmon (Salmo salar L.) against infectious pancreatic necrosis, while vaccine-mediated protection is unaffected. *J. Fish Dis.* **42**, 1271–1282 (2019).

40. Johansson, L. H., Timmerhaus, G., Afanasyev, S., Jørgensen, S. M. & Krasnov, A.

Smoltification and seawater transfer of Atlantic salmon (Salmo salar L.) is associated with systemic repression of the immune transcriptome. *Fish Shellfish Immunol.* **58**, 33–41 (2016).

41. Nuñez-Ortiz, N. *et al.* Atlantic salmon post-smolts adapted for a longer time to seawater develop an effective humoral and cellular immune response against Salmonid alphavirus. *Fish Shellfish Immunol.* **82**, 579–590 (2018).

42. Lee, S.-Y. & Eom, Y.-B. Analysis of Microbial Composition Associated with Freshwater and Seawater. *Biomed. Sci. Lett.* **22**, 150–159 (2016).

43. Wang, Y. *et al.* Comparison of the levels of bacterial diversity in freshwater, intertidal wetland, and marine sediments by using millions of illumina tags. *Appl. Environ. Microbiol.* **78**, 8264–8271 (2012).

44. Scheiermann, C., Gibbs, J., Ince, L. & Loudon, A. Clocking in to immunity. *Nature Reviews Immunology* vol. 18 423–437 (2018).

45. Matson, K. J. E. *et al.* Isolation of adult spinal cord nuclei for massively parallel single-nucleus RNA sequencing. *J. Vis. Exp.* **2018**, 1–12 (2018).

Material and Methods

Animal welfare statement

The Atlantic salmon smoltification experiment was conducted as part of the routine, smolt production at Kårvik havbruksstasjonen, approved by the Norwegian Animal Research Authority (NARA) for the maintenance of stock animals for experiments on salmonids. This is in accordance with Norwegian and European legislation on animal research.

Experimental Design

Atlantic salmon (*Salmo salar*, Aquagene commercial stain) were raised from hatching in freshwater, under continuous light (LL, > 200 lux at water surface) at ambient temperature (~10^{o}C). Juvenile salmon were housed in 500 L circular tanks and fed continuously with pelleted salmon feed (Skretting, Stavanger, Norway). At seven months of age parr (mean weight 49.5g) were sampled for T1 (experiment start). Two days later remaining parr were equally distributed between two 100L circular tanks, and over the next seven days the photoperiod was incrementally reduced to a short photoperiod (SP, 8h light:16h darkness). T2 sampling occurred on experimental day 53 (44 days on SP), remaining parr were transferred back to LL on experimental day 60. T3 sampling occurred on experimental day 110 (50 days after return to LL), then a sub-cohort of fish were netted out and transferred to full strength seawater for 24h before the final T4 collection.

RNAseq Analysis

Gill samples were collected, RNA extracted and libraries prepared, sequenced and mapped as Iversen et al (2020). Raw counts were analysed using EdgeR (ver. 3.30.0), using R (ver. 4.0.2) and RStudio (ver. 1.1.456). An ANOVA-like test was used to identify differential expressed genes between T1-T3 samples. Clustering analysis was performed using Pearson correlation, and heapmaps rendered using the R package pheatmap. An exact test was performed to identify differential expressed genes between T3 and T4.

Single nuclei RNAseq Analysis

Gills for single nuclei analysis were collected on dry ice and stored at -80^{o}C. Duplicate samples were processed for T1-T4. Nuclei were released by detergent mechanical lysis, then samples were homogenized (30s) and nuclei isolated by sucrose gradient [45]. Libraries were created

using Chromium Single Cell 3' GEM, Library & Gel Bead Kit v3 (10x technologies) by University of Manchester genomic technology core facility (UK). Raw data was converted to counts per cell using Cell Ranger (10x Technologies, ver. 3.1.0) and processed using NCBI annotations. The R package Seurat (ver. 3.1.5) was used to perform an integrated analysis using all snRNAseq data [24], further details in results and discussion. Raw data will be available following peer-reviewed publication.

Acknowledgements

The authors thank all of the animal staff at Kårvik havbruksstasjonen for their expert care of the research animals, and the University of Manchester Genomics Technology core facility (UK) for performing chromium 10x library preparation for snRNAseq. ACW is supported by the Tromsø forskningsstiftelse (TFS) grant awarded to DGH (TFS2016DH). The Sentinel North Transdisciplinary Research Program Université Laval and UiT awarded to DGH supports this work. SHW is supported a grant from the Tromsø forskningsstiftelse (TFS) starter grant TFS2016SW. Experimental costs were covered by HFSP grant "Evolution of seasonal timers" RGP0030 /2015 awarded to ASIL and DGH.

Author Contributions

Conceptualization, A.C.W., Y.M., E.H.J., A.S.I.L and D.G.H; Resources, A.C.W, Y.M and M.I.; Investigation, A.C.W., Y.M., M.I. E.H.J and D.G.H; Formal Analysis, A.C.W, Y.M., L.M.I., T.N and S.R.S; Visualization, A.C.W and S.H.W; Writing – Original Draft, A.C.W and S.H.W; Writing –

Review & Editing, All; Supervision, A.S.I.L and D.G.H; Project Administration, A.S.I.L and D.G.H; Funding Acquisition, A.S.I.L and D.G.H.

Figure Legends

Figure 1. Single nuclei RNAseq analysis of Atlantic salmon gill tissue. A) Gill tissue processing. B) UMAP plot of pooled cell data from 18844 cells representing eight samples from four collection states. The plot indicates 20 separate cell clusters. C) Expression of marker genes in 20 cell clusters. From left to right: hierarchical relatedness of difference cell clusters; total cells in each cluster; UMI number in each cell cluster; gene features in each cell cluster; violin plots showing expression pattern of marker genes for each cluster. Abbreviations: ACs - accessory cells, DCs - dendritic cells, ECs - epithelial cells, fib - fibrocytes, GCs - goblet cells, LECs - lymphatic endothelial cells, MCs - myeloid cells, MRC - mitochondrion-rich cells, NDCs - non-differentiated cells, PVCs, pavement cells, RBCs - red blood cells (erythrocytes), TCs - T cells, VCs - vascular cells.

Figure 2. Comparative abundance of cell clusters at different sampling points. A) Experimental design. Fish were kept in constant light (LL) from hatching then transferred to short photoperiod (SP; 8L:16D) for 8 weeks before being returned to constant light (LL) for 8 weeks. Finally the fish were transferred to sea water for 24h. Sample points are indicated T1-T4. B) Subset of cell clusters from T2, T3 and T4 (green and red dots) overlaid on T1 cells (grey dots). C) Increasing abundance of sea-water mitochondrion-rich cells (MRCs SW) and vascular cells (VC 3) during smoltification C) Decreasing abundance of leukocytes and immune-associated cells during smoltification.

Figure 3. Photoperiodic changes in gill gene expression and localized cell cluster expression. A) Heat map representing 9746 genes differentially regulated (FDR <0.01) from T1-T3. Regulatory patterns for 5 major cluster are shown as amplitude index and 95% confidence limits. Major gene ontology terms for each cluster are shown. B) RNAseq data for "classical" smoltification-related genes and violin plots showing their cluster specific expression.

Figure 4. Sea-water transfer-associated changes in gill gene expression and localized cell cluster expression. A) Genes differentially regulated (FDR <0.01) by 24h seawater transfer. Major gene ontology terms for each cluster are shown. B) RNAseq data for sea-water transfer-related genes and violin plots showing their cluster specific expression.

Supplemental Figure 1. RNAseq data for winter-dependent genes and violin plots showing their cluster specific expression.

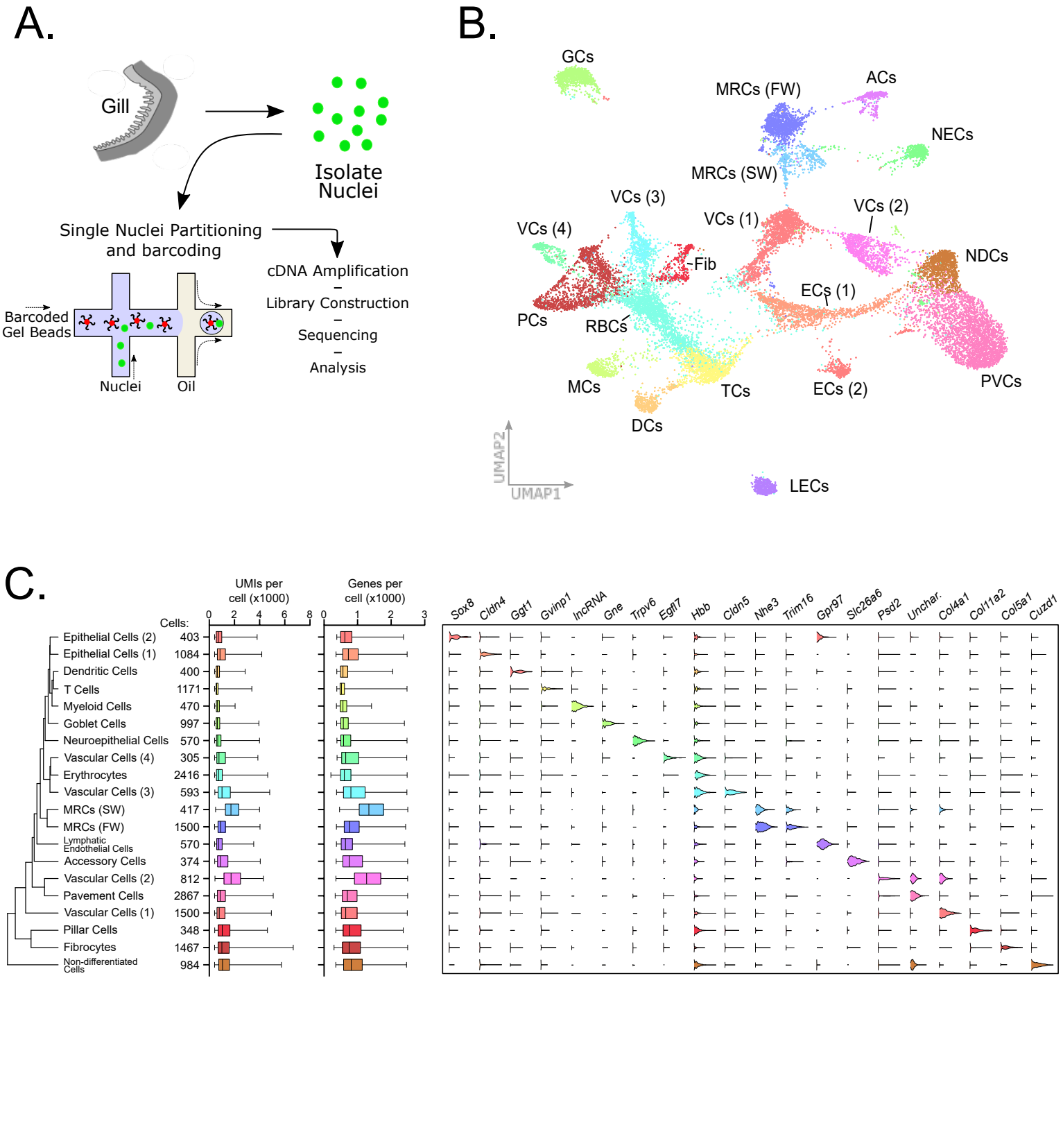

Figure 1.

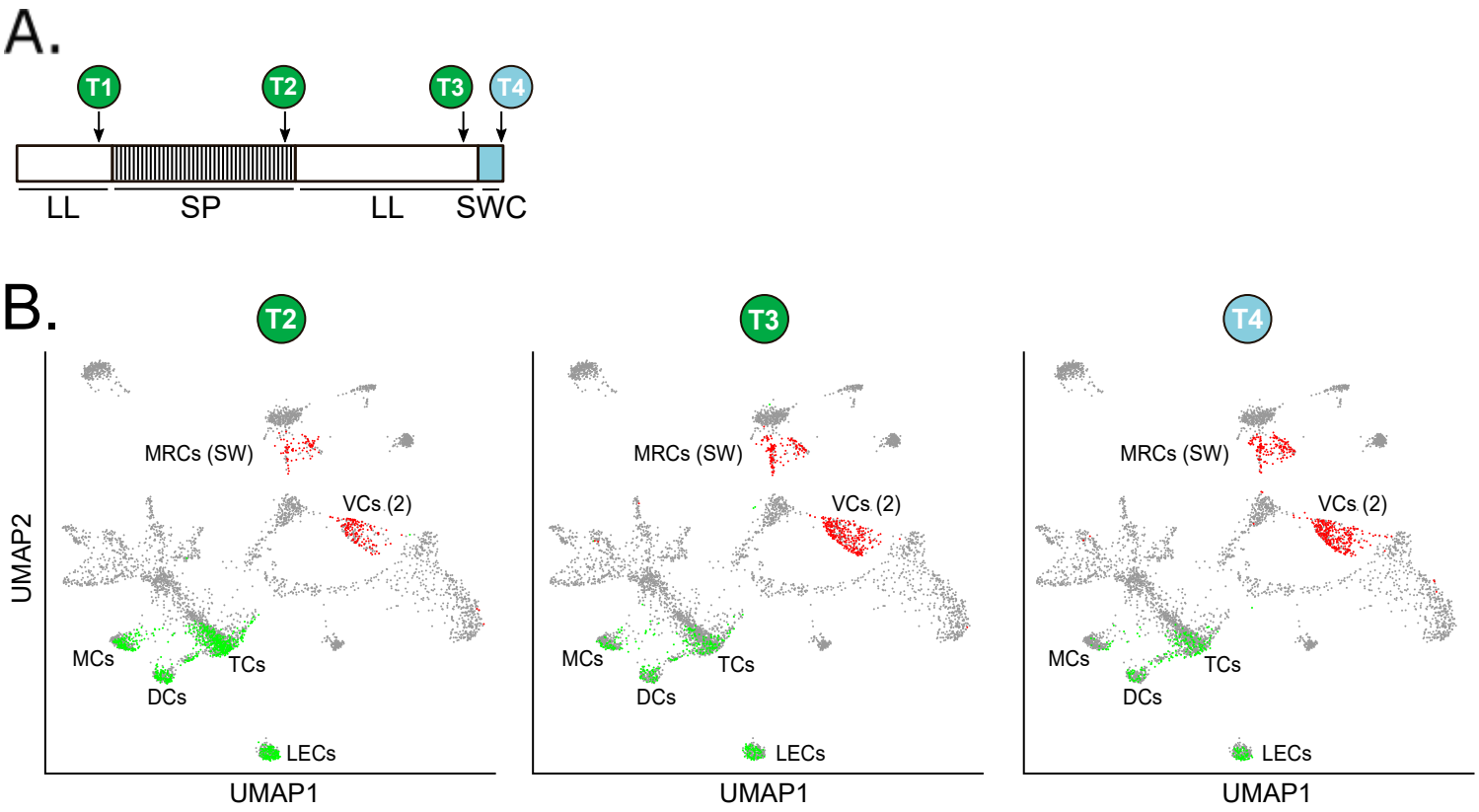

Figure 2.

A.

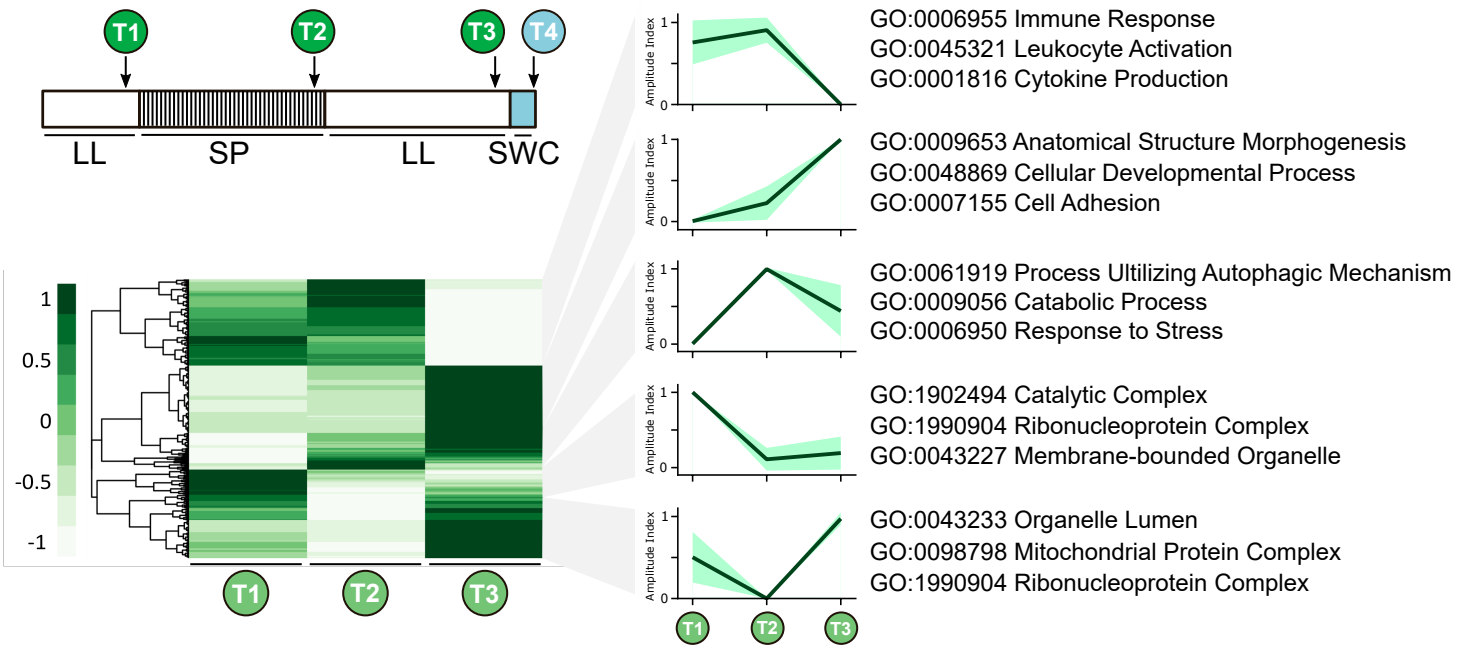

B.

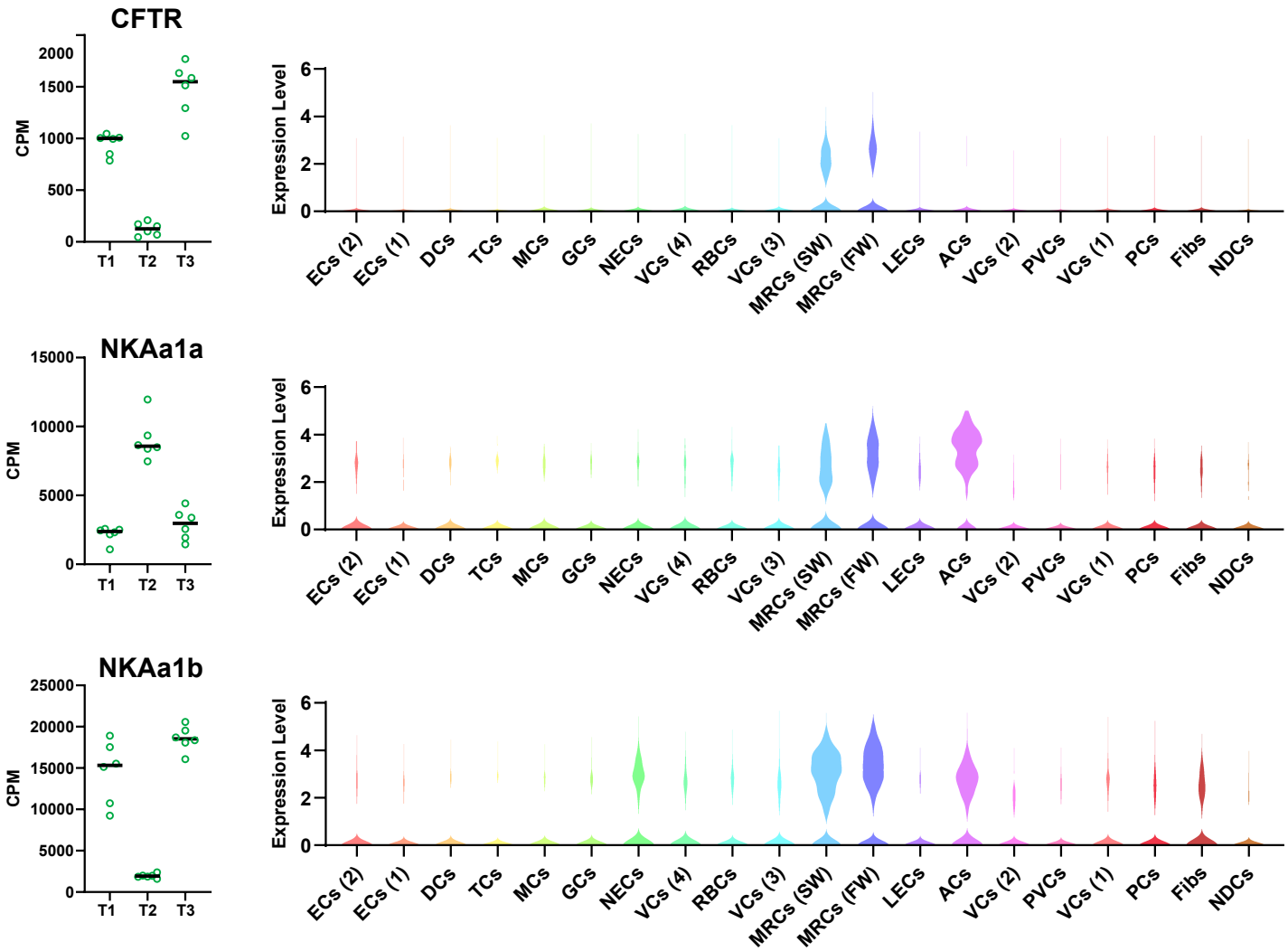

Figure 3.

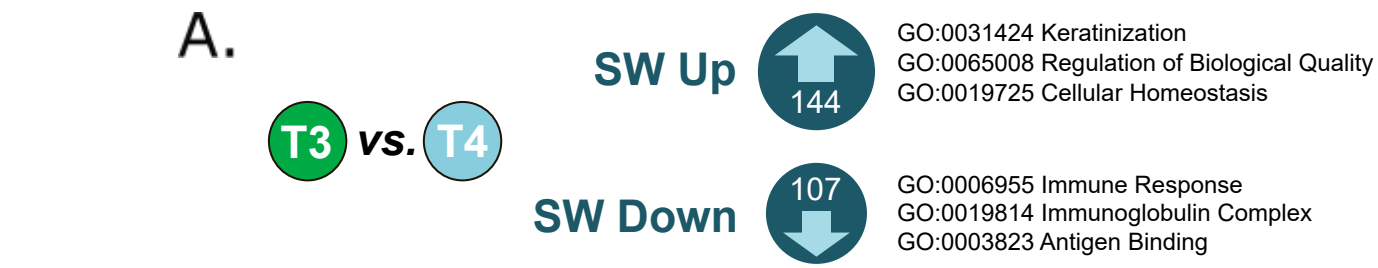

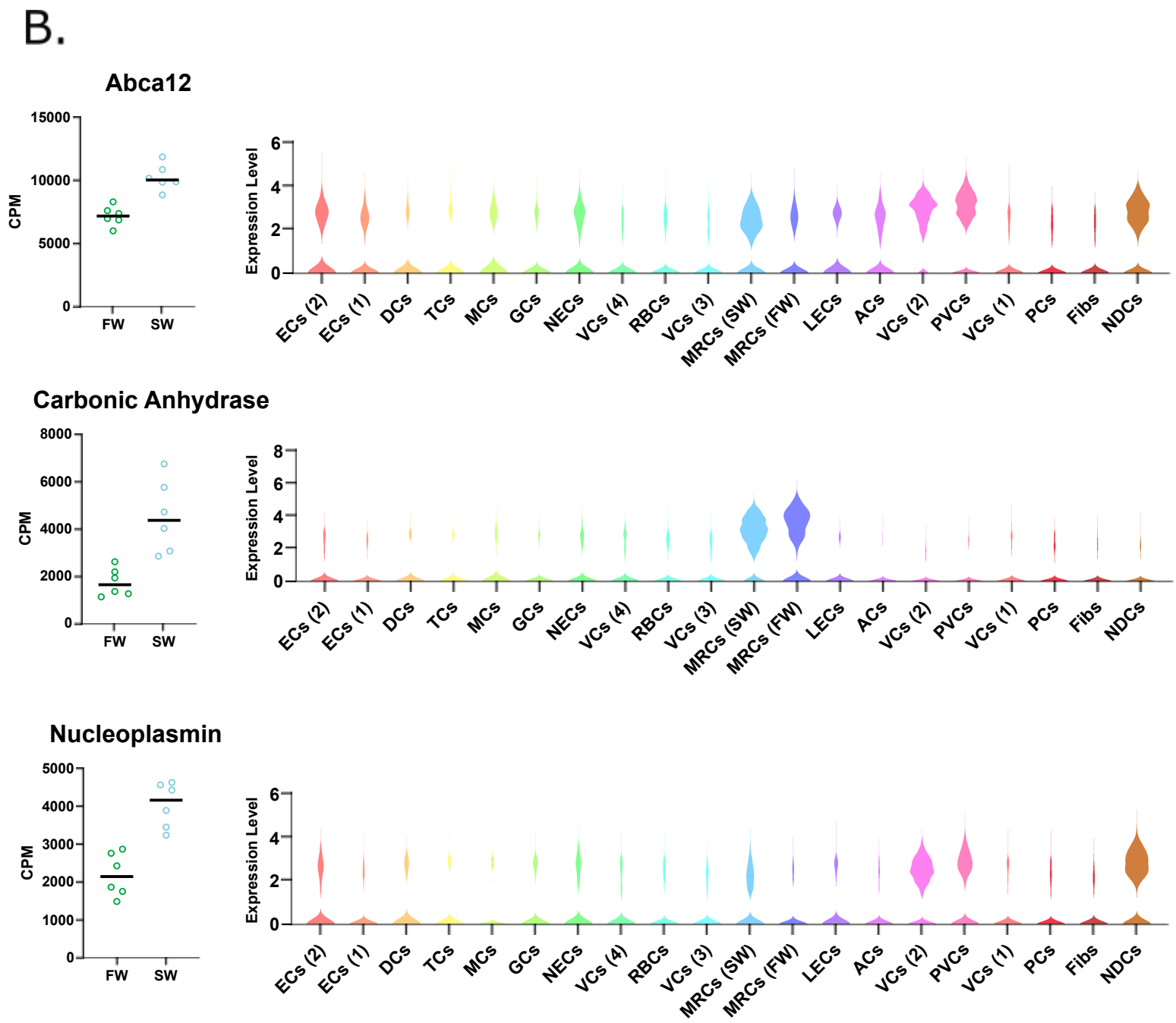

Figure 4.